

A Frequency-Space Approach for Motion Correction in functional MRI

Vince Calhoun^{*§}, Tulay Adali[§], Godfrey Pearlson^{*}

^{*}Johns Hopkins University Div. of Psychiatric Neuro-Imaging, Baltimore, MD

[§]University of Maryland Baltimore County Dept. of Electrical Engineering, Baltimore, MD

Abstract

The registration of the temporal images acquired during a functional MRI experiment is a necessary step to ensure accurate activation images. Large data sets and off-line image reconstruction suggest 1) the need for efficient algorithms, 2) the importance of minimizing registration errors, 3) an advantage to be gained by working in the native MR k-space domain. We present the extension of a non-iterative frequency based registration algorithm and then compare it with a well-known iterative image based algorithm gauging the relative merits of each with special application to functional MRI data. Fourier methods are utilized to decouple the rotation and translation components during detection, minimize interpolation artifacts in registration by using the shift-theorem and rotation by shearing, and to take advantage of the native MR data space by incorporating it into the off-line reconstruction stage. It is shown that the new method is efficient, highly reliable, does not require an initial condition/threshold setting and did not appear to suffer from local minima for the S/N of a typical fMRI experiment.

1) Introduction

Magnetic resonance imaging (MRI) is increasingly being utilized to explore the physiology or the function of the brain by repeatedly imaging a particular region over time, using a pulse sequence sensitive to changes in blood flow or blood oxygenation. Activations on the order of 2-5% at 1.5 Tesla may be observed by subtracting the "on" state from the "off" state or by applying statistical tests such as a correlation with an ideal waveform to provide a measure of the reliability of the results.

The small signal makes it especially important for the analysis of the results to incorporate the potential of motion between the temporal images or volumes acquired. This motion is comprised of 1) head motion between scans, 2) physiologic motions such as brain motion during the cardiac cycle or respiration. It may be further complicated by the non-homogeneous magnetic properties of the head as well as the system inhomogeneities in the static field B_0 or the rotating radio-frequency magnetic field B_1 . Out-of-plane motion during the imaging also interferes with the established steady state in

tissue magnetization. In addition, motion may be correlated with the stimulus and so a correction algorithm should tease this out without misregistering on the stimulus. Large amounts of data are acquired routinely (two thousand slices of 128×128 voxels not unusual). If a volumetric data set is acquired, there are four dimensions to consider. Hence, a rapid method of correction is also desirable. While incorporating all the effects of motion probably calls for a non-linear solution, it is clear that there are some components requiring additional information about spin-history and phase, e.g. navigator echo. Because of reduced processing cost over non-linear solutions and good empirical correction we adopt a linear approach. The head motion is intra-subject, and as such, prescribes itself readily to a rigid-body solution. A practical approach then is to use a rigid-body correction to gain the speed advantage and reduce the effect of head motion while attempting to quantify the benefits of the methodology. We present an approach to rigid-body correction living primarily in frequency-space and compare it with an approach in image-space (AIR)[1] while gauging their relative merits as applied to functional MRI data. This method builds on a frequency-based algorithm, decoupled automated rotational and translational registration (DART)[2]. We describe the theory for each method then present a series of experiments designed to compare these two methods. Several enhancements to the DART algorithm are incorporated such as 1) the use of the log magnitude to increase sensitivity to high frequency components for rotation, 2) sub-pixel accuracy is obtained for both rotation and translation via an extraction and zero-filling method, 3) rotation is performed by applying 1-D shears, 4) direct k-space application through incorporation of the registration process into the reconstruction stage. In addition, the expansion of the algorithm to three dimensions is discussed in theory, implementation results will be available at the conference.

2) Theory

DART is a frequency based algorithm which exploits in the frequency domain the decoupling of rotation and translation to derive an efficient scheme for registration. A rotation translates into a rotation

about the origin and by the Fourier shift theorem a translation becomes a phase shift (multiplication by a complex exponential function). Thus, if one could determine the rotation-angle of the transform and correct the original images, then only a phase shift would remain which would in turn reveal the relative translations, correctable by multiplication in the Fourier domain by a complex exponential. The DART algorithm performs the rotation correction by regridding the k-space data.

The DART Algorithm is more historically an application of a symmetric phase-only matched filter (SPOMF) in a rotation and translation invariant manner[3],[4]. We incorporate the advantage of working directly in k-space and in addition, the computational load is decreased, as we don't use Fourier regridding. Sub-pixel accuracy is achieved by extracting a neighborhood about the correlation peak and by taking the FFT, zero-filling and applying the inverse FFT. Rotation of the data set also utilizes the shift-theorem by using shears applied via 1D FFTs phase shifted by the index and weighted by the shear factor. In determination of the angle of rotation, the log-magnitude image is re-coded into polar coordinates to improve determination of the rotation angle.

Given two images, a test image a and a target or template t the SPOMF algorithm may be succinctly described via the notation in Equation 1

$$\mathfrak{F}^{-1} \left(\frac{\mathfrak{F}\{a\} \cdot \mathfrak{F}^*\{t\}}{|\mathfrak{F}\{a\}| \cdot |\mathfrak{F}\{t\}|} \right)$$

Equation 1: The standard SPOMF Algorithm

which corresponds to a spatial correlation. The normalization of the images sharpens the selectivity of the correlation since the spectral phase preserves the location of objects but is insensitive to the image energy. The complex conjugate of the target image will result in the elimination of similar phase components and what is left will be the phase difference.

The phase difference is due solely to the spatial translations, Δx , Δy ignoring noise and assuming identical images. Transforming back into the spatial domain will then result in an image that has a peak at the location of the translation. An example of this is seen in Figure 1 through the maximum location along the x direction.

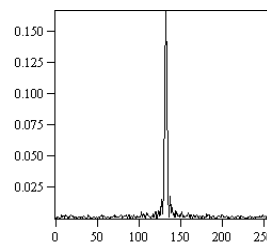


Figure 1 : A typical SPOMF correlation peak illustrating the high sensitivity of this method

This same algorithm may also be used to determine the rotation coordinate if the Fourier

transform of both the test and the target images is first resampled into polar coordinates. Taking the magnitude of each resampled image eliminates the phase shift associated with a translation. The rotation will then correspond to a phase shift along the θ direction. Taking the log of the image, i.e., $\log(1 + |\mathfrak{F}\{a_{\text{polar}}\}|)$ increases the information provided by the high frequencies. In addition, since we are using magnitude information and the magnitude is of course symmetrical, the polar-recoding scheme will only work uniquely for angles in the range $[0,180]$ degrees. Applying the SPOMF algorithm will then provide the rotation angle. So the proper implementation of this entire algorithm is, to first determine the rotational component and correct it and to determine the translation components and correct for them.

Correction of both the translation and rotation components is done via Fourier methods. The translation correction is performed by multiplying the Fourier transform of the test image by a complex exponential $e^{i(\Delta x^*x + \Delta y^*y)}$ to cancel the phase shift induced by the Δx and Δy values. Correction of the rotation is implemented via shearing using a 1D Fourier transform weighted by the shear factor[5] in the row direction, the column direction, and the row direction, respectively. Using three shears corresponds to applying a rotation matrix in 2D (Equation 2).

$$\begin{pmatrix} \cos \theta & -\sin \theta \\ \sin \theta & \cos \theta \end{pmatrix} = \begin{pmatrix} 1 & -\tan \frac{\theta}{2} \\ 0 & -1 \end{pmatrix} \begin{pmatrix} 1 & 0 \\ \sin \theta & 1 \end{pmatrix} \begin{pmatrix} 1 & -\tan \frac{\theta}{2} \\ 0 & 1 \end{pmatrix}$$

Equation 2: A 2D rotation matrix produced from the product of three shear matrices (the shear weights are typed in bold)

AIR[1] is an iterative procedure offering a 3-8 parameter linear model in 2D or 6-15 parameters in 3D. It uses as its cost function either the least squares of the two images or the normalized variance of the two-way division of the images. The premise of the second cost-function is that when the two images match exactly, the division will be 1 at all points. The second method has the advantage of being insensitive to scaling differences although there is also an option to use least squares with intensity re-scaling. When implementing the images, a threshold value must be set to determine what information to include in the sample-space. Everything above the threshold is included. The threshold requirement thus introduces a scaling sensitivity to the cost functions. Other necessary parameters are the sampling density and decrement ratio. These parameters can result in a large

difference in output results depending upon whether the iteration locates a local minimum.

Extension to 3D

The SPOMF algorithm is then extended to 3D by using 3D Fourier Transforms, using $e^{i(\Delta x * x + \Delta y * y + \Delta z * z)}$ as the phase correction for translation, and by recoding the log magnitude Fourier Transform into spherical coordinates. Resolution in the third dimension is typically much lower (eg 6-20 slices) and if standard efficient Fourier methods are desired a power of two is preferable and can be achieved by zero filling the data or algorithms not dependent upon this restriction must be used. The shearing technique is observed to be still useful, but the number of shears increases since both θ and ϕ are variable in 3D whereas only θ must be estimated in 2D. The computational workload increases considerably, but since rotation and translation are independent in frequency space no iteration is needed. Incorporation of the 3D registration into the reconstruction phase provides additional efficiencies. Thus, the efficiency of the algorithm is still desirable.



Figure 2: Simulation results for rotation (1st & 2nd rows) and translation (3rd & 4th rows). Numbering by column and starting from the left are 1) the target images, 2) test minus target, 3) test minus untransformed target, 4) the AIR result, 5) the SPOMF result, 6) AIR minus SPOMF

3) Studies & Results

Simulated Motion

Test images were created by using two contiguous slices of a 3D MRI spoiled-GRASS image with one of the slices being translated by +4 voxels in the x direction and +15 voxels in the y direction or rotated by 10 degrees. The contiguous slices were used to create a noise signature between the two images. The original images and difference images show very similar corrections for the AIR and the SPOMF algorithms as observed in Figure 2. Upon closer inspection the SPOMF images show slightly less edge difference and a slightly more homogeneous appearance intracranially.

Phantoms

A Grapefruit phantom and a human brain embedded in gelatin were prepared and rotated or translated through 40 increments of 0.25-0.5 mm and 0.25-0.5 degrees, respectively. The rotations were not about the center of the image. The raw k-space data was acquired. In the case of the grapefruit, a partial k-space acquisition was used and it was reconstructed using a Homodyne reconstruction scheme.[6] A “longitudinal” view of both is presented in Figure 3 with the observance of a misregistration in the AIR rotational data. This can be corrected by modifying the threshold, changing sampling scheme and/or tightening the iterations, but it was fairly typical to find several

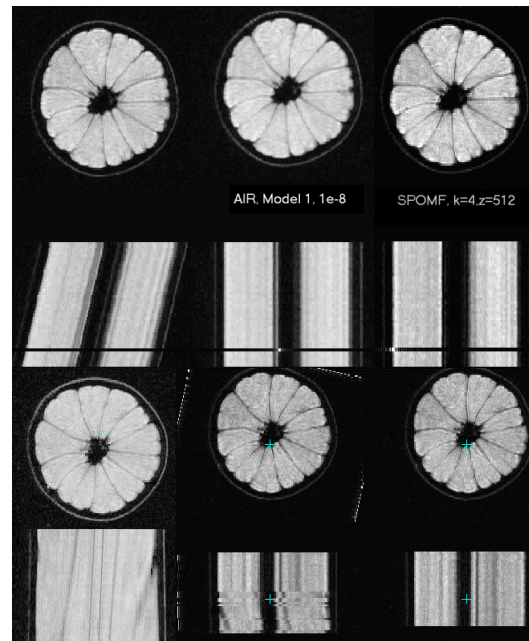


Figure 3: Translation and rotation phantom data by column for 1) uncorrected, 2) AIR, 3) SPOMF data. Note the effect of registration errors that need to be carefully monitored for the AIR algorithm.

slices misregistered each time. The black slice is due to an acquisition error by the MR scanner.

This same data is displayed in Figure 4 for the difference of two particular slices in Figure 3 with a final difference between the SPOMF and the AIR algorithms in the final column. Again, they perform very similarly, although there are some observable non-homogeneous differences as indicated by the differential image. In all cases, sinc interpolation was used to reslice for the AIR algorithm as bilinear interpolation resulted in a marked decrease in accuracy compared with the SPOMF algorithm. This same experiment was also performed using a brain hemisphere embedded in gelatin. These results are not displayed here due to space limitations.

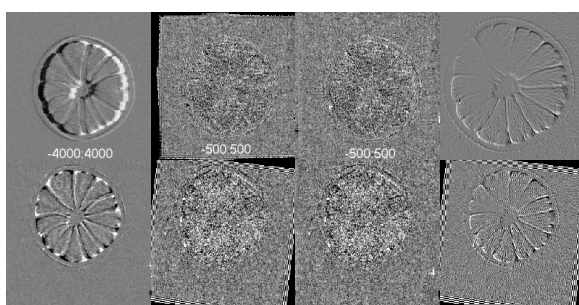


Figure 4: Difference images for a phantom study for translation (row 1) and rotation (row 2). The columns represent 1) uncorrected differences, 2) AIR, 3) SPOMF, 4) AIR minus SPOMF.

Human fMRI Study

An fMRI study consisting of 220 images and involving stimulation of the visual cortex is presented in Figure 5. The difference of two images reveals a slight motion artifact. Application of the AIR and SPOMF algorithms reduces the motion and upon closer inspection, the lateral edges appear to be reduced slightly more by the AIR algorithm while

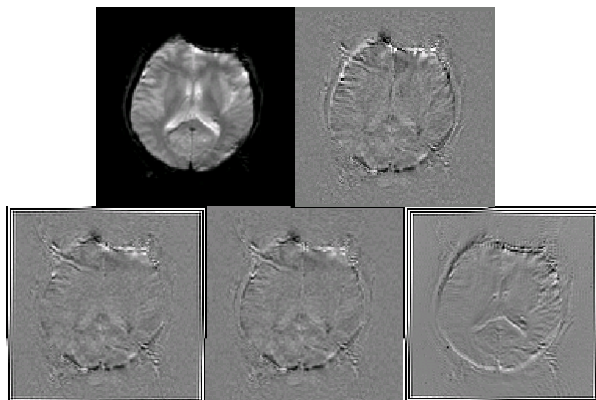


Figure 5: Difference images from an fMRI experiment with small but visible motion. The columns are 1) original slice, 2) difference image, 3) AIR, 4) SPOMF, 5) AIR minus SPOMF.

the wide frontal edges appear to be reduced more by the SPOMF algorithm.

We have quantified the results from these studies with a variety of measures including least-squares, variance, and noise distribution characterizations. In addition, the phantom results were compared with the expected results and the two correction algorithms. The SPOMF appears to perform at least as well as AIR and slightly better at times. It has the additional advantages of efficiency due to a) incorporation into image reconstruction and b) decoupling of rotation and translation, c) no initial condition, d) reduced misregistration, e) excellent interpolative properties, and thus is a desirable methodology.

Additional comparisons include a detailed analysis of the effect of each motion-correction algorithm on the statistical maps (a simple t-test in our case). Due to the small signal differences (2-5% at 1.5T) this is a crucial determinant of the registration method chosen. Speed benchmarks of each method are performed for a typical fMRI dataset. The 3D implementation is tested and compared with the 3D AIR algorithm in the same manner as the 2D comparison.

References

- [1] RP Woods, JC Mazziotta, SR Cherry, "MRI-PET Registration with Automated Algorithm", *Journal of Computer Assisted Tomography*, vol. 17 no. 4, pp. 536-545, 1993.
- [2] LC Maas, B Frederick, P Renshaw, "Decoupled Automated Rotational and Translational Registration for Functional MRI time Series Data: The DART Registration Algorithm", *MRM* vol.37, pp. 131-139, 1997.
- [3] Q Chen, M Defrise, F Deconinck, "Symmetric Phase-Only Matched Filtering of Fourier-Mellin Transforms for Images Registration and Recognition", *IEEE Trans. On Pattern Analysis and Machine Intelligence*, vol. 16, no. 12, pp. 1156-1168, 1994.
- [4] G Ritter, J Wilson, Handbook of Computer Vision Algorithms in Image Algebra, chapt. 9, CRC Press, Inc., 1996.
- [5] W Eddy, M Fitzgerald, D Noll, "Improved Image Registration by Using Fourier Interpolation", *MRM* vol. 36, pp. 923-931, 1996.
- [6] D Noll, DG Nishimura, A Macovski, "Homodyne Detection in Magnetic Resonance Imaging", *IEEE Tran. On Medical Imaging*, vol. 10, no. 2, pp. 154-163, 1991.